Acta Crystallographica Section B
Structural Science
ISSN 0108-7681

Superspace crystal symmetry of thermoelectric misfit cobalt oxides and predicted structural models

D. Grebille,[a]* H. Muguerra,[a] O. Pérez,[a] E. Guilmeau,[a,b] H. Rousselière[a] and R. Funahashi[c]

[a]CRISMAT-ENSICAEN Laboratory, UMR CNRS 6508, 6 Bd Maréchal Juin, 14050 Caen CEDEX, France, [b]Laboratory of Structural Inorganic Chemistry, University of Liège, Chemistry Department B6, Sart-Tilman, B4000 Liège, Belgium, and [c]National Institute of Advanced Industrial Science and Technology, Midori-gaoka, Ikeda, Osaka 563-8577, Japan

Correspondence e-mail: dominique.grebille@ensicaen.fr

Received 2 November 2006
Accepted 15 March 2007

Single crystals of thermoelectric misfit lamellar cobalt oxide phases in the Bi–Ca–Co–O and I–Bi–Ca–Co–O systems were synthesized. They are characterized by aperiodic structures involving two partially independent sublattices: a CdI_2-type pseudohexagonal CoO_2 layer and a rocksalt-type $BiCaO_2$ slab allowing the intercalation of iodine. The crystal symmetry of these structures is discussed using the four-dimensional superspace formalism. The superspace Laue classes of the iodine-free and the intercalated compounds are $P2/m(0\delta\frac{1}{2})$ ($a_1 = 4.901$, $b_1 = 4.730$, $b_2 = 2.80$, $c_1 = 14.66$ Å, $\beta = 93.49^\circ$) and $A2/m(0\delta1)$ ($a'_1 = 4.903$, $b'_1 = 4.742$, $c'_1 = 36.51$ Å, $\beta = 87.30^\circ$), respectively. A comparison is given with the related Bi–Sr–Co–O misfit compounds. The present structures are compatible with the presence of an intrinsic modulation with a wavelength matching the misfit aperiodicity in the **b** direction. Preliminary partial structure refinements confirm the layer stacking of the structure and the intercalation of I between the Bi—O layers for the second phase. A comparison with other cobalt oxide phases, as well as symmetry and metric considerations allow us to predict average structures for these new phases and to describe the common structural features assumed for all these lamellar misfit cobalt oxides.

1. Introduction

Layered cobalt oxides are materials well known for their promising thermoelectric properties (Terasaki *et al.*, 1997; Li *et al.*, 1999; Funahashi *et al.*, 2000; Maignan, Hébert, Pi, Pelloquin, Martin, Michel, Hervieu & Raveau, 2002). Beside this physical interest, all these compounds present very close structural relationships, including the presence of pseudo-hexagonal layers (CoO_2) consisting of edge-sharing CoO_6 octahedra (Miyazaki, 2004; Morita *et al.*, 2004). Between these layers, various rock-salt type layers can be intercalated: Ca–Co–O (Lambert *et al.*, 2001), Bi–Sr–Co–O (Hervieu *et al.*, 1999), Tl–Sr–Co–O (Hébert *et al.*, 2001), Pb–Sr–Co–O (Pelloquin *et al.*, 2002), Sr–Co–O (Nagaï *et al.*, 2006). The so-called misfit structure results from the regular stacking of these partially independent systems, which share two periodicities, but which present different, and incommensurate, periodicities in the third direction (generally chosen as the **b** direction). The corresponding ratio $\delta = b_1/b_2$ characterizes the aperiodicity of the structure and is responsible for an intrinsic non-stoichiometry of the compounds, resulting from the mismatch between the structural slabs.

From the crystallographic point of view, these phases are very interesting for their surprising variety of structural models, related to the different types of rock-salt slabs. For a proper structural description, the superspace formalism for aperiodic structures (Janssen *et al.*, 1992; van Smaalen, 2004) is

needed for the determination of the global crystal symmetry of the studied phase, including generalized Laue classes, reflection conditions and space groups. Similar misfit structures are also present in sulfide and selenide compounds and structure refinements were also developed in this superspace approach (van Smaalen, 1992). This step is made easier using single-crystal diffraction data. The structure can then be refined using adequate structural parameters including average positions and mutually modulated displacements (Leligny *et al.*, 2000; Lambert *et al.*, 2001).

The Bi–Ca–Co–O and I–Bi–Ca–Co–O systems were recently investigated (Funahashi *et al.*, 2005; Guilmeau *et al.*, 2007), in which similar structural features could be recognized involving new aperiodicities. The preliminary crystal-symmetry determinations of two new phases are presented here. Structural models are deduced from the comparison with known structures of related compounds, in agreement with the proposed crystal symmetry. A discussion of physical properties is presented elsewhere (Guilmeau *et al.*, 2005, 2007).

2. Experimental

Single crystals were grown by the flux method, using Bi_2O_3, $CaCO_3$ and Co_3O_4 powders as precursors. The precursors were mixed with a cationic ratio of Bi:Ca:Co = 2.5:2.5:2 and heated at 1123 K for 50 h. The resulting powder was ground and heated again under the same conditions. The resulting powder was then mixed with Bi_2O_3 powder (weight ratio of 1:0.5), heated in an alumina crucible at 1323 K for 20 h and then cooled down to 973 K (cooling rate 2 K h^{-1}).

Iodine intercalated specimens were obtained when single-crystal samples were placed under vacuum in a sealed glass tube with an excess of iodine, then heated at 393 K for 50 h. The composition and the iodine content were both measured by wavelength-dispersive spectroscopy (WDS). Several crystals were analyzed and their composition was found to be homogenous. The calcium atomic composition is set as a reference to 2 in the following. The composition was averaged from more than 800 measurements on several crystals and showed a very weak cationic ratio dispersion: $Bi_{1.65\ (3)}Ca_{2.00\ (4)}Co_{1.47\ (4)}Al_{0.22\ (2)}O_x$. These analyses provide evidence for a deficiency in Bi and Co, but also for the presence of Al because of contamination from the crucible. The corresponding phase will be referred to as BCCO in the following sections. The intercalated single-crystal samples (IBCCO) are characterized by an iodine content which is very close to 1.

Large platelet-like single-crystal samples ($\simeq 3 \times 3$ mm^2) were selected and they were mounted for reflection Bragg–Brentano 2θ–ω scans on a two-circle diffractometer (Rigaku RINT–TTR). Cu $K\alpha$ radiation was used to measure the $(00l)$ reflections. These samples are characterized by a large mosaicity and were too large for transmission X-ray diffraction experiments. Smaller samples ($\simeq 0.5 \times 0.5$ mm^2) were selected for a global data collection with a four-circle Nonius KappaCCD diffractometer using Mo $K\alpha$ radiation for cell and crystal symmetry determination. The large mosaicity did not allow us to determine a satisfactory set of integrated intensities, but lattice parameters and crystal symmetry could be determined from digitally reconstructed precession images, generated from the measured data by *EVALCCD* software (Duisenberg *et al.*, 2003).

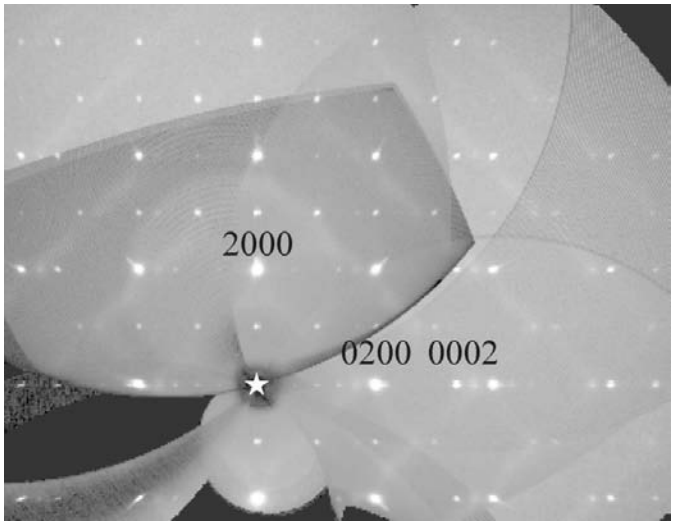

Figure 1
Reconstructed $(hk0)$ reciprocal plane of the $[BiCaO_2]_2[CoO_2]_{1.69}$ compound. The indexing is given with the H, K, L, M quadruplet (see text).

3. Structural model and stacking scheme

Reconstructed precession images of the pristine BCCO phase are in agreement with the expected misfit character of the structure. The diffraction pattern is characterized by two monoclinic lattices sharing the same periodicities **a** and **c**, but showing two independent periodicities along **b**, b_1 and b_2 (Fig. 1): $a = 4.9013\ (7)$, $b_1 = 4.730\ (1)$, $b_2 = 2.80\ (1)$, $c = 14.661\ (2)$ Å, $\beta = 93°49\ (2)'$. The $\delta = b_1/b_2$ value (1.69) is close to the corresponding values observed in the $[Ca_2CoO_3][CoO_2]_\delta$ family (CCO phase hereafter; Masset *et al.*, 2000; Lambert *et al.*, 2001; Karppinen *et al.*, 2004). It differs slightly from the same ratio in the Pb–Sr–Co–Rh–O (from 1.67 to 1.79; Pelloquin *et al.*, 2005), the Bi–Pb–Sr–Co (from 1.86 to 1.92; Yamamoto *et al.*, 2002), the Tl–Sr–Co–O (from 1.76 to 1.79; Maignan, Wang, Hébert, Pelloquin & Raveau, 2002) or in the Pb–(Sr,Ca)–Co–O systems (from 1.61 to 1.79; Maignan, Hébert, Pelloquin, Michel & Hejtmanek, 2002). The small differences observed for δ can be easily explained by the corresponding difference in ionic radii. According to all the previous structural studies, the first subsystem lattice is a distorted rocksalt-type lattice which can accommodate different atomic species, resulting in different b_1 values and the second subsystem lattice is related to the CoO_2 layers, which are systematically present in all these structures with a single b_2 value (2.80 Å). In particular, the present stoichiometry and the observed value of δ are compatible with the chemical formula $[Bi_{0.83}CaO_2]_2[Co_{0.84}Al_{0.16}O_2]_{1.69}$ which can be compared with the related compound

Table 1
Refined structural parameters from data collection from the four-circle diffractometer experiment.

	BCCO		IBCCO		
	z	u (10^{-4} Å^{-2})	Occupancy	z	u (10^{-4} Å^{-2})
Co	0	14 (14)	0.84	0	78 (37)
O1	0.0704 (1)	−48 (36)	0.84	0.055 (2)	95 (100)
Ca	0.1963 (4)	40 (18)	1	0.1613 (7)	81 (40)
O2	0.242 (3)	282 (137)	1	0.194 (5)	272 (250)
Bi	0.3842 (2)	66 (9)	1	0.3106 (3)	147 (21)
O3	0.370 (4)	458 (430)	1	0.282 (10)	387 (460)
I	–	–	0.96 (4)	0.5	273 (42)

$[Bi_{0.87}SrO_2]_2[CoO_2]_{1.82}$ (BSCO phase hereafter; Leligny *et al.*, 2000). Owing to these clear analogies and to the similar values of the stacking parameters ($2c$ = 29.32 Å for BCCO against 29.86 Å for BSCO, the corresponding contraction can be explained by steric differences between Ca^{2+} and Sr^{2+}), a first model for BCCO based on the BSCO structure has been considered in this work, but should also be compatible with the observed crystal symmetry.

Unfortunately, a complete structure refinement is not possible because of the poor crystal quality of our samples; the only reliable data mainly concern the (00l) reflections and thus are related to the z coordinates of the atoms. Thus, a confirmation of the stacking scheme corresponding to the average structural stacking model for the BCCO samples is expected.

A first refinement was performed using 21 (00l) reflections ($5 \leq l \leq 25$) obtained from the four-circle diffractometer data collection. The data were corrected for Lorentz–polarization and absorption, assuming a platelet like morphology, using the *JANA*2000 software (Petříček & Dušek, 2000). Preliminary z coordinates were obtained from the structure of $[Bi_{0.87}SrO_2]_2[CoO_2]_{1.82}$. Only the z coordinates of the atoms and their isotropic Debye–Waller parameters were refined towards a good agreement factor (R = 0.0254, wR = 0.0295). The final structural parameters are given in Table 1. They do not differ significantly from the corresponding initial values. These results were also used for a profile-fitting refinement of the two-circle data, with a specific Lorentz and overspill correction, taking into account a small single crystal totally irradiated by the incident beam, in reflection mode. The agreement is also close (R = 0.0439, wR = 0.0294, R_p = 0.0585, R_{wp} = 0.0852; Guilmeau *et al.*, 2007). Both refinements are consistent with each other and clearly confirm the stacking model.

Dealing with the even poorer IBCCO single crystal, a cell could still be refined using the *EvalCCD* and *NDIRAX* software: a_1 = 4.903 (1), b_1 = 4.742 (4), b_2 = 2.80, c_1 = 18.305 (9) Å, β = 94.99 (3)°. The values are close to those of BCCO, except for the considerable increase in the c parameter. A similar expansion of the c axis of around 3.6 Å was already observed in iodine-intercalated $Bi_2(Sr,Ca)_2Co_2O_x$ whiskers (Funahashi *et al.*, 2005) or $Bi_2Sr_2CaCu_2O_8$ cuprate phases (Xiang *et al.*, 1990, 1992; Subramanian, 1994). It was interpreted as an intercalation of a new I layer between the two neighbouring BiO layers. A preliminary model was generated by keeping all the previous interlayer distances constant, except for BiO–BiO, and by adding an iodine layer at z = 0.5, with a free occupation parameter. This model was then refined on 11 (00l) reflections using only the z coordinates, isotropic Debye–Waller parameters and the occupancy of the I site. Good agreement factors were obtained for the two data sets (Table 1; Guilmeau *et al.*, 2007; R = 0.0276, wR = 0.0295 for the four-circle and R = 0.0253, wR = 0.0175, R_p = 0.0707, R_{wp} = 0.111 for the two-circle diffractometer data, respectively). The refined occupation of the I site gives a Bi:Ca:I ratio of 1.9:2.00:0.96, almost equal to the WDS analyses.

From these partial crystal structures it is possible to calculate the different interlayer distances and compare them with other layered structures. The refined thicknesses of the CoO_2 layers are nearly identical in the two structures (2.06 and 2.01 Å, respectively, for BCCO and IBCCO) and they are comparable to the corresponding values of other layered cobalt oxides (2.00, 2.01, 2.02 and 1.97 Å for $[Bi_{0.87}SrO_2]_2[CoO_2]_{1.82}$ (Leligny *et al.*, 2000), $[Ca_2CoO_3]$-$[CoO_2]_{1.62}$ (Grebille *et al.*, 2004) and $[Ca_2CoO_3][CoO_2]_{1.62}$ polytypes (Lambert *et al.*, 2001), and Na_xCoO_2 (Balsys & Davis, 1996; Jorgensen *et al.*, 2003), respectively). In the hydrated superconducting compounds $Na_xCoO_{2-y}H_2O$, the corresponding thickness is significantly smaller: 1.94 (Lynn *et al.*, 2003), 1.85 (Jorgensen *et al.*, 2003) and 1.77 Å (Takada *et al.*, 2003). Thus, the thermoelectric oxides probably share the same CoO_2 layer, with the same structural configuration and same Co environment. The Ca, Co and Bi layers also show the same interlayer distances in both structures (Ca—Co 2.87 against 2.95 Å; Bi—Ca 2.75 against 2.73 Å). Consequently, the difference in c parameters is due to the intercalation of I and results in a larger Bi–Bi interlayer distance (6.91 in IBCCO against 3.39 Å in BCCO). For the BCCO compound, the BiO–BiO interlayer distance is equivalent to the corresponding ones in the high T_c superconducting cuprate phases: 3.15 ($Bi_2Sr_2CaCu_2O_{8+\delta}$; Grebille *et al.*, 1996), 3.37 ($Bi_{2-x}Pb_x$-$Sr_2CaCu_2O_{8+\delta}$; Jakubowicz *et al.*, 2001) or 3.32 Å ($Bi_{2+x}Sr_{3-x}Fe_2O_{9+\delta}$; Pérez *et al.*, 1995).

4. Crystal symmetry

4.1. Crystal symmetry of the pristine BCCO sample

According to the partial structure refinements, the BCCO and BSCO structures are closely related. Let us compare their crystal symmetry as it can be deduced from their diffraction patterns.

BSCO was proven to be I centered [superspace symmetry group $I2/a(0\delta0)$; Leligny *et al.*, 2000]. The first subsystem ($Bi_{0.87}SrO_2$) displays an intrinsic modulation of the planar monoclinic type characterized by a **q** vector: $0.293\mathbf{a}^* + 0.915\mathbf{c}^*$. This modulation, orthogonal to the misfit direction, is characterized by large longitudinal atomic displacements within the double BiO structural layers.

The (hk0) planes of the diffraction patterns of BCCO (Fig. 1) and BSCO (Fig. 1 in Leligny *et al.*, 2000) are similar, disregarding the difference between the respective b_1 para-

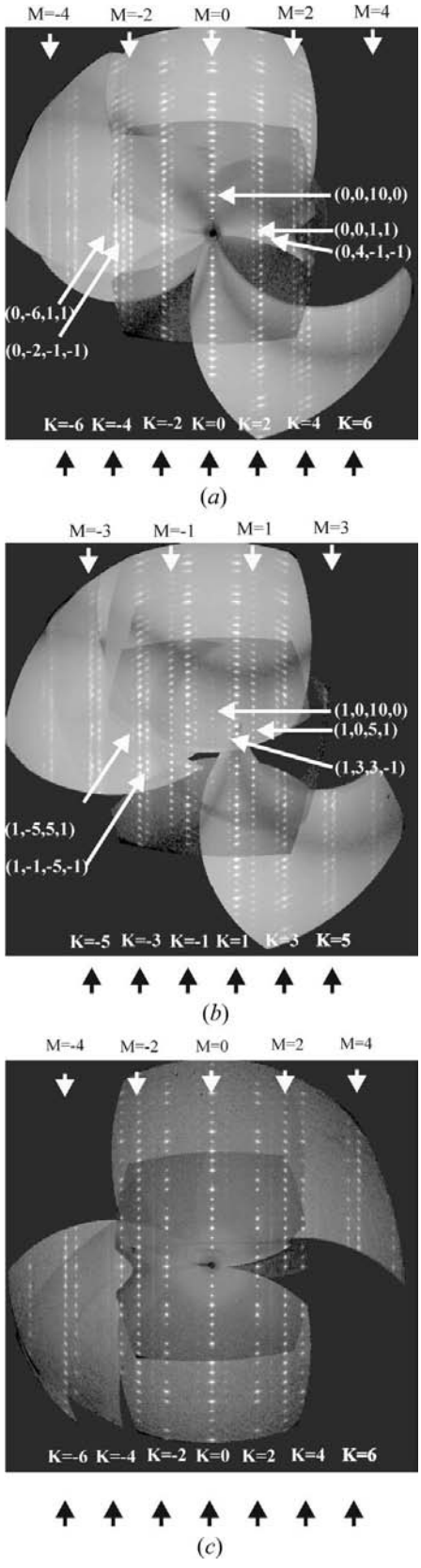

Figure 2
Reconstructed (*a*) (0*kl*) and (*b*) (1*kl*) reciprocal planes of the $[BiCaO_2]_2[CoO_2]_{1.69}$ compound. The indexing is given with the H, K, L, M quadruplet (see text). (*c*) (0*kl*) reciprocal planes of $[Ca_2CoO_3][CoO_2]_{1.652}$.

meters. However, careful inspection of the diffraction patterns shows that for BCCO the lattice of the first subsystem is only compatible with a primitive cell (Fig. 1), while the lattice of the second subsystem is consistent with an A centered cell with a double c parameter (Figs. 2*a* and *b*). The satellite reflections, for example in the (0*kl*), (1*kl*) or (2*kl*) planes, can all be indexed using the wavevector $\mathbf{q} = (b_1/b_2)\mathbf{b}_1^*$ which is compatible with the misfit character of the structure, but no extra satellite reflections can be observed in the (*h*0*l*) plane. Nevertheless, a comparison of the (0*kl*) diffraction planes of BCCO (Fig. 2*a*) and CCO (Fig. 2*c*), and (*h*0*l*) of BSCO (Fig. 2 in Leligny *et al.*, 2000) shows a strong analogy (in position and in intensity) between the satellite reflections observed around the main reflections of the first subsystem in BCCO and those associated with the intrinsic modulation evidenced in BSCO. This type of satellite reflections is absent for CCO. They can be associated with the presence of BiO layers and one can suppose that an intrinsic modulation, analogous to those of BSCO or of Bi–Cu superconducting oxides, is also present in BCCO, but shares both the direction and the periodicity of the misfit behaviour. There is here a probable mutual lock-in of these two aperiodicities on each other. A proper and complete structure refinement is needed to confirm this point.

In order to ensure the compatibility between the two sublattices, one can describe the global lattice of the misfit structure using the superspace symmetry developed for aperiodic structures (Janssen *et al.*, 1992) and index all the reflections with four indices. Then, choosing $\mathbf{a}_1$, $\mathbf{b}_1$ and $\mathbf{c}_1$ as the basis vectors for subsystem 1 and $\mathbf{a}_2 = \mathbf{a}_1$, $\mathbf{b}_2 = \mathbf{b}_1/\delta$ and $\mathbf{c}_2 = 2\mathbf{c}_1$ as the basis vectors for subsystem 2, all reflections can be indexed by

$$\mathbf{S} = h_1\mathbf{a}_1^* + k_1\mathbf{b}_1^* + l_1\mathbf{c}_1^* + m\mathbf{q}^* \tag{1}$$

with

$$\mathbf{q}^* = \mathbf{b}_2^* + \mathbf{c}_2^* = \delta\mathbf{b}_1^* + \mathbf{c}_1^*/2. \tag{2}$$

The corresponding superspace Laue class is $P2/m(0\delta\frac{1}{2})$. This can equivalently be expressed as

$$\mathbf{S} = H\mathbf{a}_1^* + K\mathbf{b}_1^* + L\mathbf{c}_2^* + M\mathbf{b}_2^* \tag{3}$$

with

$$H + H_1,\ K = k_1,\ L = 2l_1 + m,\ M = m. \tag{4}$$

The following reflection condition is then obeyed

$$HKLM:\ L + M = 2n. \tag{5}$$

The main reflections for subsystem 1 are characterized by $M = m = 0$ and the reflection condition reduces to $HKL0$: $L = 2n$, which justifies the original choice of the c_1 parameter for this lattice. The main reflections for subsystem 2 are characterized by $K = 0$, and the reflection condition is consistent with the observed A centering of the basic structure lattice of subsystem 2. All reflections including all satellite reflections can be indexed using the (H, K, L, M) indices of (3) and (4). This indexing has been chosen in the figures.

4.2. Crystal symmetry of iodine-intercalated IBCCO crystals

Precession images were computationally reconstructed from the frames measured on the I-intercalated crystals. They exhibit a strong analogy with the precession images of BCCO, except for the larger c parameter (Figs. 3 and 4). Note that the larger mosaicity of IBCCO is probably related to increased stacking disorder and larger misorientations of the layers in these very flexible lamellar samples (observed by electron microscopy; Guilmeau *et al.*, 2007).

The refinement of the unit cell from the collected data leads to C-centered monoclinic unit cells for both subsystems [a_1 = 4.903 (1), b_1 = 4.742 (4), b_2 = 2.80, c_1 = 18.305 (9) Å, β = 94.99 (3)°]. The comparison between the ($0kl$) and ($1kl$) planes (Fig. 5) of the BCCO and IBCCO compounds shows strong analogies. As previously mentioned, the satellite reflections ($K \neq 0$ and $M \neq 0$) are simultaneously consistent with the misfit periodicity (*i.e.* the b_1/b_2 ratio) and an intrinsic modulation of the rocksalt-type sublattice. Considering for IBCCO (Fig. 5*b*) the (a_1, b_1, b_2, c_1) unit cell, the location of the satellite reflections corresponding to the intrinsic modulation requires the same modulation wavevector as for BCCO: $\mathbf{q} = \delta\mathbf{b}_1^* + \mathbf{c}_1^*/2$. However, the C centering of the basic structure unit cell of IBCCO is not compatible with the $\mathbf{c}_1^*/2$ part of $\mathbf{q}$ and the symmetry of the second sublattice. A careful comparison of Figs. 5(*a*) and (*b*) shows the different location along c^* of the reflections of BCCO and IBCCO [see the relative positions of the two sets of reflections ($K = 0$, $M = 1$) and ($K = 1$, $M = 0$)]. The main reflections of the second sublattice cannot be interpreted in the present case as satellite reflections of the first one, as they should. Moreover, some extra weak reflections, *e.g.* the ($10l$) reflections in Fig. 4(*b*), are not compatible with the C centering condition. The indexing of ($10l$) and of all the satellite reflections involves a doubling of the $\mathbf{c}_1$ parameter. Following these different observations, a new monoclinic cell can be defined (Fig. 4*b*)

$$\begin{aligned}\mathbf{a}_1'^* &= \mathbf{a}_1^* - \mathbf{c}_1^*/2\\ \mathbf{b}_1'^* &= \mathbf{b}_1^*\\ \mathbf{c}_1'^* &= \mathbf{c}_1^*/2\end{aligned} \tag{6}$$

one finds a_1' = 4.903, b_1' = 4.742, c_1' = 36.51 Å and β' = 87.30°. All reflections can then be indexed using

$$\mathbf{S} = h_1\mathbf{a}_1'^* + k_1\mathbf{b}_1'^* + l_1\mathbf{c}_1'^* + m\mathbf{q} \text{ with } \mathbf{q}'^* = \mathbf{b}_2'^* + \mathbf{c}_2'^* = \delta\mathbf{b}_1'^* + \mathbf{c}_1'^*. \tag{7}$$

The general reflection condition $k_1 + l_1 = 2n$ is now obeyed, corresponding to an A centering. For the second subsystem, the main reflections can be expressed as

$$\mathbf{S}_2 = h_2\mathbf{a}_1'^* + k_2\mathbf{b}_2'^* + l_2\mathbf{c}_2'^*. \tag{8}$$

They correspond to $h_2 = h_1$, $k_1 = 0$, $k_2 = m$ and $l_2 = l_1 + m$. The condition $k_1 = 0$ implies $l_1 = 2n$ and consequently $k_2 + l_2 = 2n'$: the second sublattice is also A centered. The corresponding superspace Laue class is $A2/m(0\delta1)$. This can be equivalently expressed as

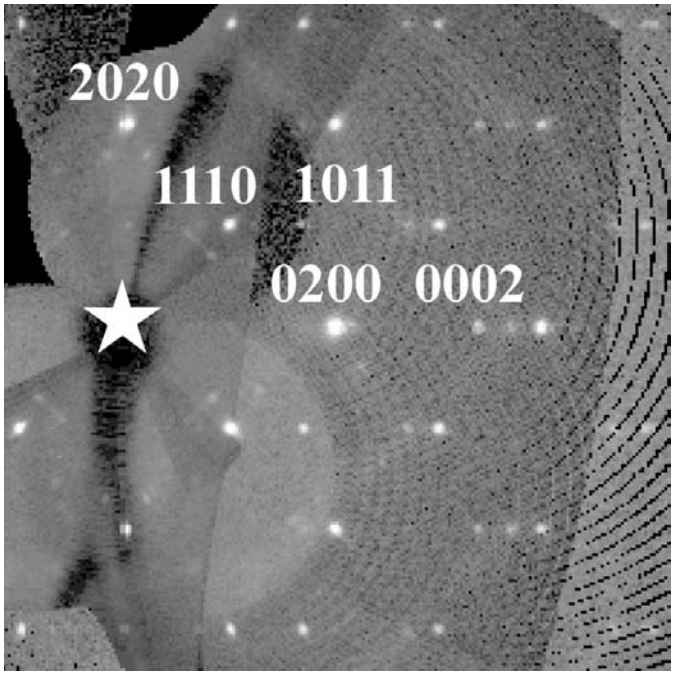

Figure 3
Reconstructed (HKH) reciprocal plane of the $I[BiCaO_2]_2[CoO_2]_{1.69}$ compound. The indexing is given with the H, K, L, M quadruplet (see text) and corresponds to the ($hk0$) reflections in the ($\mathbf{b}_1^*$, $\mathbf{b}_1^*$, $\mathbf{c}_1^*$) initial monoclinic cell.

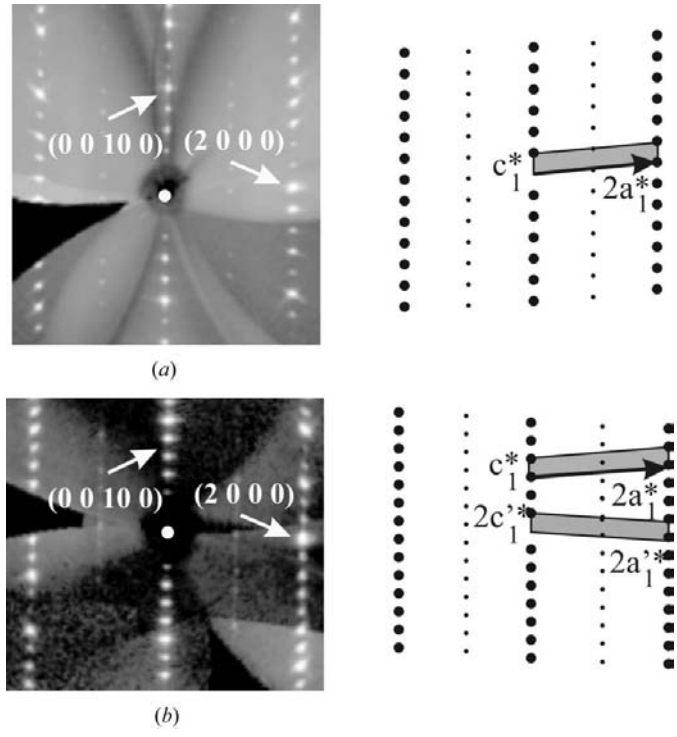

Figure 4
Reconstructed ($h0l$) reciprocal planes (*a*) of the $[BiCaO_2]_2[CoO_2]_{1.69}$ and (*b*) $I[BiCaO_2]_2[CoO_2]_{1.69}$ compounds. The indexing is given with the H, K, L, M quadruplet (see text). A schematic representation of the corresponding reciprocal spaces is given within the two cell assumptions for (*b*).

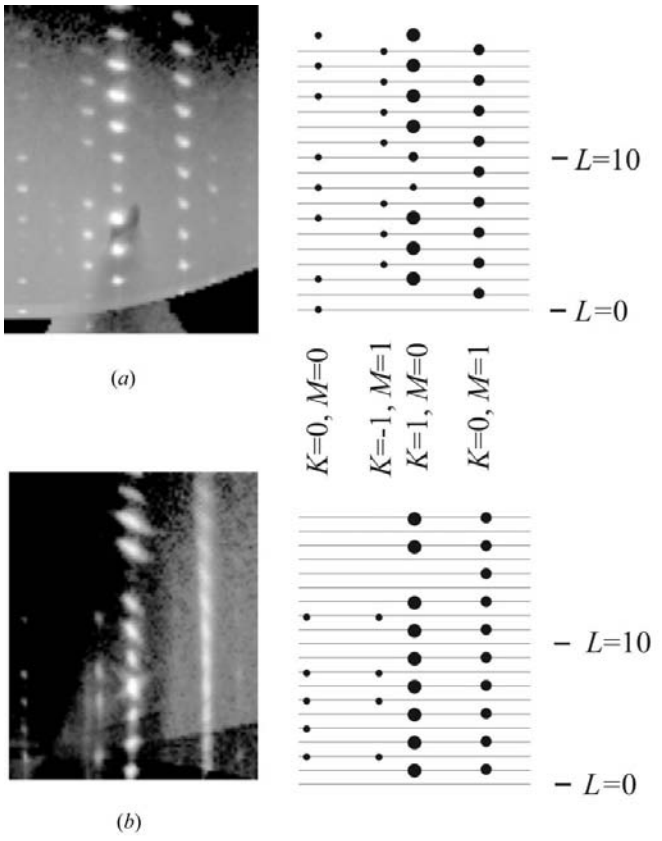

Figure 5
Reconstructed ($1kl$) reciprocal planes (a) of the $[BiCaO_2]_2[CoO_2]_{1.69}$ and (b) $I[BiCaO_2]_2[CoO_2]_{1.69}$ compounds. The indexing is given with the H, K, L, M quadruplet (see text).

$$\mathbf{S} = H\mathbf{a}_1'^* + K\mathbf{b}_1'^* + L\mathbf{c}_1'^* + M\mathbf{b}_2'^* \text{ with}$$
$$H = h_1,\ K = k_1,\ L = l_1 + m,\ M = m. \qquad (9)$$

The following condition is then valid: $HKLM$: $K + L + M = 2n$. The main reflections of subsystem 1 are characterized by $M = m = 0$ and the reflection condition reduces to $K + L = 2n$. The main reflections of subsystem 2 are characterized by $K = 0$ and $L + M = 2n$. All reflections can be indexed using the indices of (9). This indexing has been chosen in the figures.

5. Structure models for BCCO and IBCCO

We have described in §4 the symmetry of the misfit phases in the Bi–Ca–Co–O and I–Bi–Ca–Co–O systems. We have seen the analogy of these phases with previously reported cobalt oxide misfit compounds in the Ca–Co–O and Bi–Sr–Co–O systems. Structures are formed by two partially independent subsystem lattices. The second subsystem is built of CoO_2 layers in all cases. Only a few of these structures were accurately refined and are now well known. We can compare the structural characteristics of the CoO_2 layers and of the stackings of the neighbouring layers of the rocksalt-type subsystems in these different structures. In Figs. 6(a) and 7(a) we present schematic representations of the average structures of CCO ($[Ca_2CoO_3][CoO_2]_{1.652}$; Grebille *et al.*, 2004) and BSCO ($[Bi_{0.87}SrO_2]_2[CoO_2]_{1.82}$; Leligny *et al.*, 2000), projected along the misfit direction **b**. In Figs. 6(b) and 7(b) we have isolated similar atomic columns in these structures, showing firstly an atomic stacking direction rigorously perpendicular to the layer plane in the rocksalt-type subsystem and secondly the mutual atomic arrangement at the junction between both types of subsystems. The monoclinic arrangement results only from this common atomic configuration between both subsubsystems, creating a relative shift between the atomic columns of two consecutive slabs of the first subsystem surrounding a CoO_2 layer. In Figs. 6(c) and 7(c) we give a schematic representation of the misfit four-dimensional symmetry, through the corresponding three-dimensional compatible symmetries of both subsystems. For CCO, the superspace group $C2/m(1, \delta, 0)s0$ implies a single $C2/m$ three-dimensional space group for both subsystems, but with a relative origin shift. For BSCO, the superspace symmetry $I2/a(\alpha 0\gamma, 0\mu 0)pmm$ is compatible with symmetries $I2/a$ and $B2/a$ for the first and second subsystems, respectively. The crystal symmetries appear to be different for the two compounds, but they are compatible with common structural and geometrical features. This can be proven by considering the specific distances and angular relations. Such characteristics are defined in Fig. 8 and the corresponding values (specific distances and angles), deduced from all the previous and present refinements, are summarized in Table 2. From these values we can easily conclude that the CoO_2 layer keeps the same configuration in all these phases and we will assume a generalization of this arrangement for BCCO and IBCCO. We could

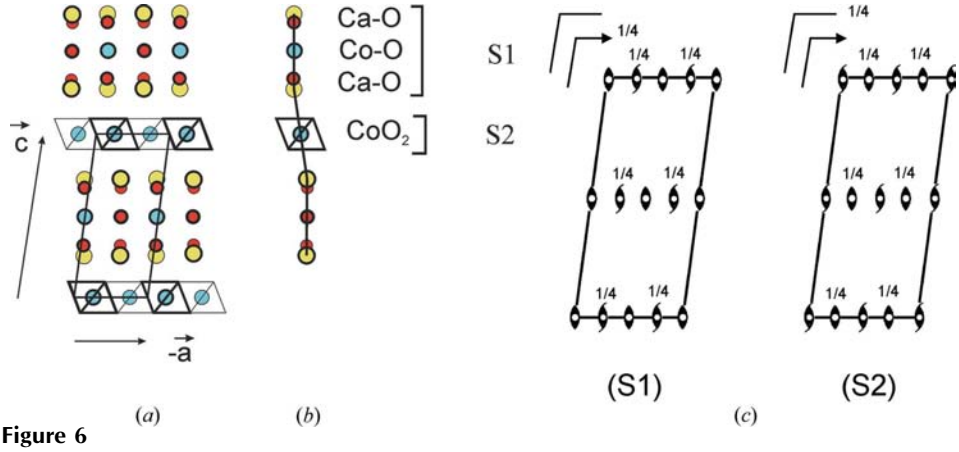

Figure 6
(a) Schematic representation of the average structure of $[Ca_2CoO_3][CoO_2]_{1.652}$ projected along **b**. (b) Atomic column characterizing the stacking mechanism of the two sublattices; S1: thick circles: $y = 0$, thin circles: $y = 0.5$; S2: thick circles: $y = -0.25$, thin circles: $y = 0.25$. (c) Schematic representation of the symmetry of the two subsystems of the misfit structure.

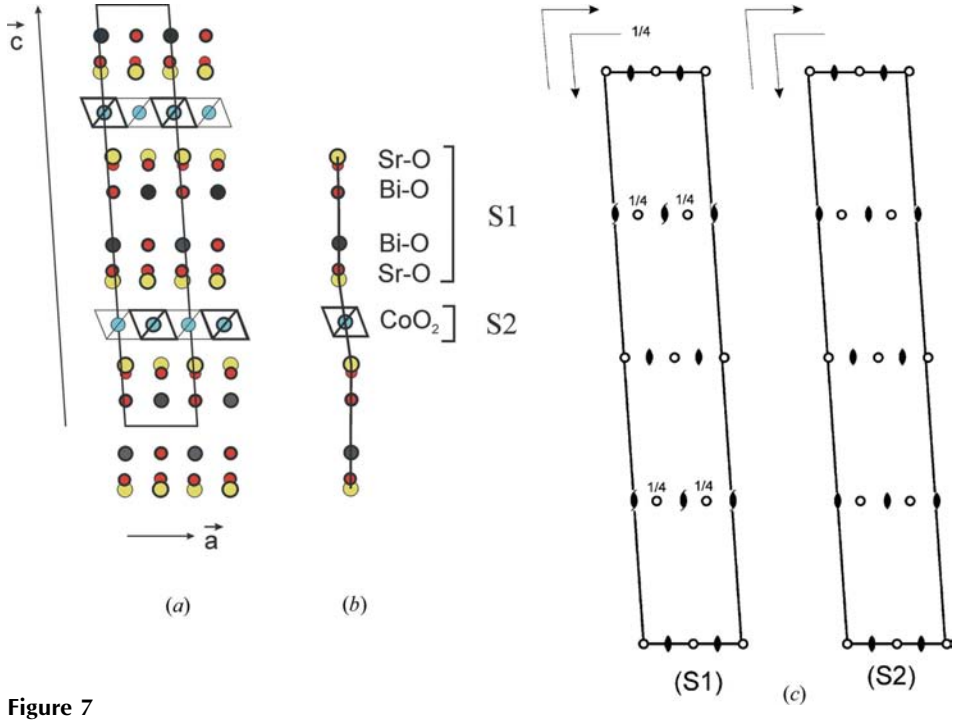

Figure 7
(*a*) Schematic representation of the average structure of $[Bi_{0.87}SrO_2]_2[CoO_2]_{1.82}$ projected along **b**. (*b*) Atomic column characterizing the stacking mechanism of the two sublattices; thick circles: $y = -0.25$, thin circles: $y = 0.25$. (*c*) Schematic representation of the symmetry of the two subsystems of the misfit structure.

still confirm this point when considering the polytype phases 2 and 3 of the CCO phase (Lambert *et al.*, 2001), which are characterized by parallel and antiparallel stackings of the CoO_2 layers. The regular alternation of the two configurations results in an orthorhombic symmetry. The same type of polytype relation involving the different possible stackings of direct or reverse monoclinic cells in a resulting monoclinic or orthorhombic cell was already discussed in the case of misfit sulfide structures (van Smaalen & de Boer, 1992). The same considerations would also be valid for the second variant identified in the BSCO phase (Leligny *et al.*, 2000). The difference with the first variant is related to an $a/2$ or $b/2$ translation of one CoO_2 layer over 2, allowing to recover a basic stacking of the two sublattices compatible with a c parameter of 14.93 Å and the superspace Laue class $C2/m(0\delta0)$. Considering only the parallel stacking of the CoO_2 layers, and assuming that the monoclinic symmetry depends only on the magnitude of the atomic shift of consecutive layers ($D \simeq 0.9$ Å), we can deduce a relation between the values of a, c and β_n of the monoclinic cell

$$\cos\beta_n = \pm(pD + na/2)/c, \quad (10)$$

where p corresponds to the number of CoO_2 layers in the unit cell and n is a relative integer allowing us to restore an eventual cell translation along **a** by switching from one atomic column in the rocksalt system to the neighbouring one. The parameter n can be chosen as a function of p and of the number of layers r in the rocksalt block. As a matter of fact, following along **c** the previously defined atomic columns (Figs. 6*b* and 7*b*), disregarding the deviation D and

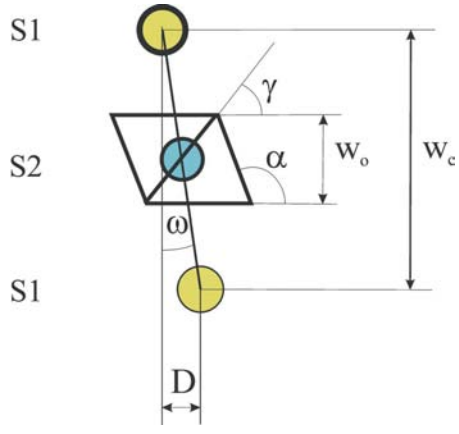

Figure 8
Geometric characteristics of the stacking of the two sublattices of a typical misfit-layered cobalt oxide structure.

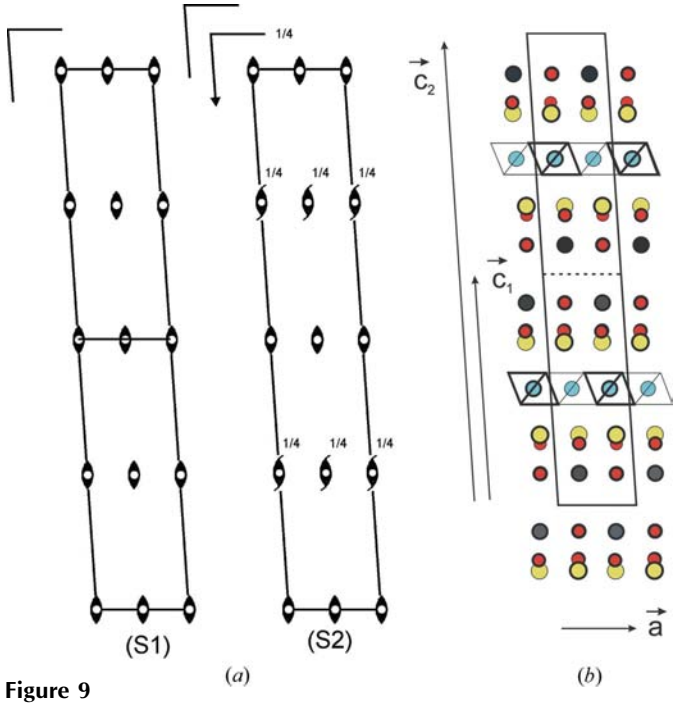

Figure 9
(*a*) Schematic representation of the basic structure symmetry of the two subsystems of $[BiCaO_2]_2[CoO_2]_{1.69}$; first hypothesis: $P2/m(0\delta_2^1)00$; (*b*) schematic representation of the corresponding proposed structural model; thick circles: $y = 0$, thin circles: $y = 0.5$.

Table 2
Comparison of interatomic distances, angles and geometrical parameters concerning the CoO_2 layer and the stacking scheme of misfit cobalt oxides (see Fig. 8).

	$[Ca_2CoO_3]$ $[CoO_2]_{1.652}$ CCO	$[Bi_{0.87}SrO_2]_2$ $[CoO_2]_{1.82}$ BSCO	$[Bi_xCaO_2]_2$ $[CoO_2]_{1.69}$ BCCO	I$[Bi_xCaO_2]_2$ $[CoO_2]_{1.69}$ IBCCO
d(Co−O) (Å)	1.89, 1.90	1.91, 1.92	–	–
d(O−O) (Å)	2.82, 2.80, 2.56	2.83, 2.81, 2.57	–	–
Angles (O−Co−O) (°)	95.5, 95.1, 84.9, 84.5	95.3, 94.8, 85.1, 84.7	–	–
α (°)	111.9	112.3	–	–
β (°)	51.0	50.7	–	–
ω (°)	8.5	9.0	–	–
W_o (Å)	2.02	2.00	2.06	2.01
W_c (Å)	5.92	6.09	5.79	5.89
$D = W_c^* \mathrm{tg}\,\omega$ (Å)	0.89	0.96	–	–

the CoO_2 layers, cations and anions of the subsystem 1 are compatible with a global rocksalt-type system: the alkaline earth atoms (or O atoms) in the atomic column just below and above the CoO_2 layer have y coordinates which differ by $\frac{1}{2}$ (Figs. 6*a* and 7*a*). As a consequence, if the number of layers r in the rocksalt-type block between two CoO_2 layers is even, two neighbouring rocksalt-type slabs are equivalent without any extra translation along **a**, and one can take n even (0, for example) to define the c cell translation. If r is odd, but p is even, then, the global number of layers in the rocksalt-type blocks of the cell is rp, an even number, and one can still take $n = 0$. On the other hand, if both r and p are odd, then rp is odd and a cation will take the place of an anion and *vice versa* in the same column. In the latter case one must take n odd (−1 or 1, for example) in order to shift to the neighbouring column of the rocksalt structure to assume the elementary lattice translation with equivalent species. Assuming a value of 0.9 Å for D, one finds $p = 1$, $r = 3$, $n = -1$, $a = 4.83$, $c = 10.83$ Å for CCO and $p = 2$, $r = 4$, $n = 0$, $a = 4.90$, $c = 29.86$ Å for BSCO. We can generalize this calculation with different misfit structures and the corresponding experimental and theoretical data are summarized in Table 3, showing very good agreement between the computed and the experimental values, validating the model and its generalization to the new compounds.

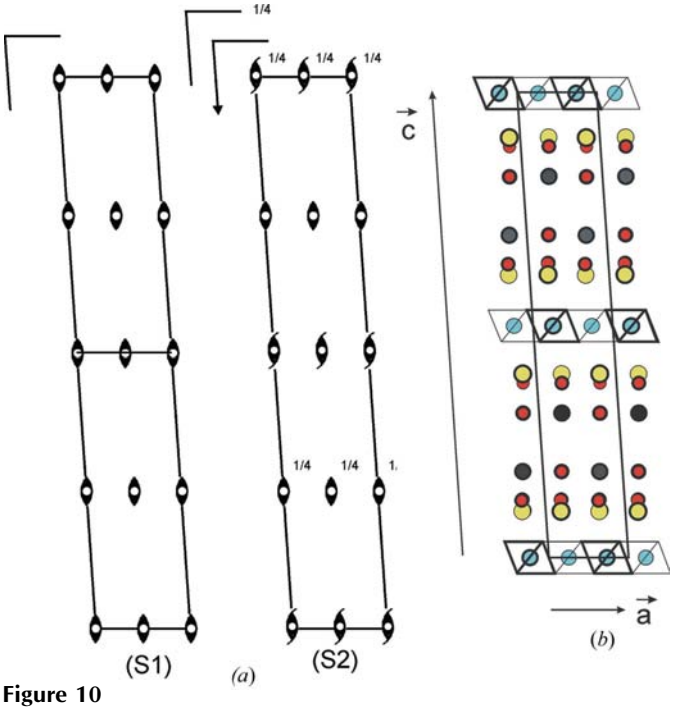

Figure 10
(*a*) Schematic representation of the basic structure symmetry of the two subsystems of $[BiCaO_2]_2[CoO_2]_{1.69}$; second hypothesis: $P2/m(0\delta\frac{1}{2})s0$; (*b*) schematic representation of the corresponding proposed structural model; S1: thick circles: $y = 0$, thin circles: $y = 0.5$; S2: thick circles: $y = -0.25$, thin circles: $y = 0.25$.

We can consider the previous metric and symmetry considerations to predict possible structures for BCCO and IBCCO. The BCCO phase and the BSCO phase ($p = 2$, $r = 4$, $n = 0$) have similar cell parameters to the BSCO phase ($p = 2$, $r = 4$, $n = 0$). One observes a slight decrease of the a, b and c parameters for subsystem 1, as a consequence of the smaller ionic radius of Ca^{2+} *versus* Sr^{2+}. Consequently, we can assume the same stacking scheme and the main difference lies in the symmetry. The observed Laue class allows two space groups: $P2/m(0\delta\frac{1}{2})00$ (first hypothesis) or $P2/m(0\delta\frac{1}{2})s0$ (second hypothesis). The corresponding schematic representations are given in Figs. 9(*a*) and 10(*a*), with the space groups $P2/m$ and $A2/m$ for the first and second subsystems, respectively. The difference between the two cases is an origin shift of the respective three-dimensional space groups of the two subsystems. One has to check now the compatibility of both symmetries with the presumed average structure of both subsystems. The pseudohexagonal layers of CoO_6 octahedra of the second subsystem are only compatible either with a $2/m$ site for the Co atom [Co atomic coordinates: 0,0,0 (respectively $0,\frac{1}{4},\frac{1}{4}$) in the first (respectively second) hypothesis], or with a Co atom at the middle point between two inversion centres and 2_1 axes of the same layer [Co atomic coordinates: $\frac{1}{4},0,\frac{1}{4}$ (respectively $\frac{1}{4},\frac{1}{4},0$) in the first (respectively second) hypothesis]. However, the model built with the Co atom on an inversion centre and building the structure with the atomic blocks as defined in Fig. 7(*b*) leads to a symmetry incompatibility with the binary axes between the BiO layers of the first subsystem. Thus, this assumption is not valid. Then, also taking into account the A centering for the second subsystem, one obtains two possible solutions as given in Figs. 9(*b*) and 10(*b*). These two models are in fact equivalent as far as the average structure is concerned, but they differ by the relationships between atomic modulated displacements of symmetry-related atoms. A structure refinement with experimental data is needed at this point for further investigations.

In the I-intercalated compound the partial refinement of the z coordinates is compatible with a central I layer between two BiO layers. The ratio Bi/I $\simeq 2$ is compatible with a new I layer in the rocksalt-type slab. We can then imagine a new atomic column as a copy of the previous ones with a supplementary I

Table 3
Comparison of experimental and theoretical β values of the different monoclinic misfit cobalt oxide structures.

Phase	a_z (Å)	c_z (Å)	p	r	n	β_n (or $180-\beta_n$)	β
CCO (Grebille *et al.*, 2004)	4.83	10.83	1	3	−1	98.04	98.13
BSCO (Leligny *et al.*, 2000)	4.905	29.86	2	4	0	93.45	93.45
BCCO (present study)	4.901	14.661	2	4	0	93.52	93.49
IBCCO (present study)	4.903	36.51	2	5	0	87.17	87.30
$[Tl_\alpha(Sr_{1-y}Ca_y)O_3][CoO_2]_{1.79}$ (Boullay *et al.*, 1998)	4.95	11.66	1	3	−1	97.76	97.76
$[Pb_{0.7}Sr_{1.9}Co_{0.4}O_3][CoO_2]_{1.8}$ (Pelloquin *et al.*, 2002)	4.938	11.525	1	3	−1	97.82	97.81
$[Ca_{0.85}OH]_2[CoO_2]_{1.72}$ (Shizuya *et al.*, 2006)	4.898	8.81	1	2	0	95.86	95.8
$[SrO]_2[CoO_2]_2$ (Nagaï *et al.*, 2006)	4.980	9.107	1	2	0	95.67	96.28
$[Ca(Co_{0.65}Cu_{0.35})O_2]_2[CoO_2]_{1.6}$ (Miyazaki *et al.*, 2002)	4.823	12.773	1	4	0	94.04	93.93
$[BiBa_{0.7}K_{0.3}O_2]_2[CoO_2]_{1.95}$ (Muguerra, 2007)†	4.94	15.57	1	4	0	93.31	93.4

† The cell parameters given in Yamauchi *et al.* (2006) concerning $[BiBaO_2]_2[CoO_2]_2$ are not relevant and should not be considered (Hervieu *et al.*, 2003)

atom (Fig. 11*a*). The lattice parameters a = 4.90 and c = 18.25 Å are compatible with monoclinic angles 87.2° (or 92.8°) for n = 0, 79.4° (or 100.6°) for n = 1 and 94.9° (or 85.1°) for n = −1 [see (10) with p = 1]. If we admit a stacking scheme equivalent to the non-intercalated BCCO compound, the intercalation of I modifies the cation–anion alternation in a column: the rocksalt-type slab is built with five layers, so that both Ca atoms in the same atomic column and the same rocksalt slab have the same y component. To recover the lattice translation in the IBCCO compound, according to the diffraction data, one needs to double the c parameter (p = 2) and we keep the same n = 0 value for the calculation of the monoclinic angle, leading to the value 87.2° for β, in agreement with the previous symmetry considerations which lead to β = 87.3° rather than the preliminary estimation of 94.99°, which would have imposed n = −1. The Laue class has been found, $A2/m(0\delta1)$, and can induce two four-dimensional superspace groups $A2/m(0\delta1)00$ (first hypothesis) and $A2/m(0\delta1)s0$ (second hypothesis; Figs. 11*b* and *c*, respectively). The corresponding three-dimensional space groups are $A2/m$ for both subsystems in both hypotheses, but with an origin shift of the lattice of the second subsystem in the second hypothesis. Trying to define the relative positions of the assumed CoO_2 layers and of the atomic columns of the rocksalt-type slab in these two cell hypotheses, two possibilities still occur for subsystem 2: either the Co atom is on a 2/m site [Co atomic coordinates: 0,0,0 (respectively $0,\frac{1}{4},\frac{1}{4}$) in the first (respectively second) hypothesis] or at the middle point between two inversion centres and 2_1 axes of the same layer [Co atomic coordinates: $\frac{1}{4},0,\frac{1}{4}$ (respectively $\frac{1}{4},\frac{1}{4},0$) in the first (respectively second) hypothesis]. Looking then at the compatible position for subsystem 1, it is possible to consider the two atomic sites for Co only in the second hypothesis. The corresponding structural models are given in Figs. 12(*a*) and (*b*).

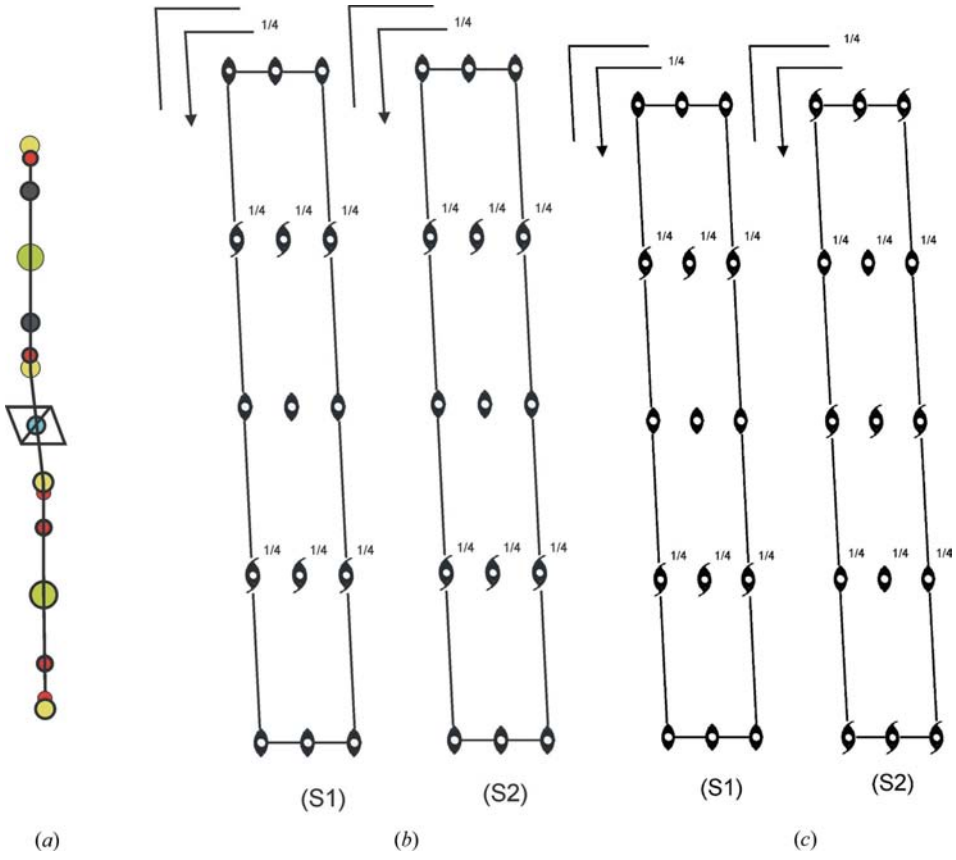

Figure 11
(*a*) Structural model for the elementary atomic column of $[IBi_2Ca_2O_4][CoO_2]_{1.69}$. (*b*) Schematic representation of the symmetry of the two subsystems in the first hypothesis $A2/m(0\delta1)00$ and (*c*) in the second hypothesis $A2/m(0\delta1)s0$.

6. Conclusion

The present single-crystal X-ray diffraction study of the misfit cobalt oxide $[Bi_{0.835}CaO_2]_2[Co_{0.87}Al_{0.13}O_2]_{1.69}$ and the corresponding I-intercalated phase outlines the very large versatility of

Table 4
Chemical composition, space group and lattice parameters of BCCO and intercalated IBCCO.

	Composition		Lattice parameters				
Compound	Bi:Ca:Co:Al:I	Space group	a (Å)	b_1 (Å)	b_2 (Å)	c (Å)	β (°)
BCCO	1.65:2:1.47:0.22:∅	$P2/m$ $(0\delta\frac{1}{2})$	4.9013 (7)	4.730 (1)	2.80	14.661 (2)	93.49 (2)
IBCCO	1.65:2:1.47:0.22:0.98	$A2/m(0\delta1)$	4.903 (1)	4.742 (4)	2.80	36.51 (2)	87.30 (3)

these structures. The substitution of Sr for Ca results in a modification of the lattice parameters for the rocksalt-type subsystem, involving a new aperiodic ratio δ. The presence of satellite reflections in the diffraction pattern is interpreted by a structural modulation, probably in relation to the Bi—O layers of the structure, as in the related Sr compound $[Bi_{0.87}SrO_2]_2[CoO_2]_{1.82}$, but now in the misfit direction. The two aperiodicities can be explained with the same δ ratio. A four-dimensional superspace Laue class $P2/m(0\delta\frac{1}{2})$ has been derived to explain the global crystal symmetry. The iodine intercalation, which has been proven to occur between the BiO layers, is responsible for a larger stacking parameter, but also for a different four-dimensional crystal symmetry $A2/m(0\delta1)$. The corresponding results are summarized in Table 4. The centering conditions are identical for the CoO_2 sublattice of both phases. The intercalated iodine only modifies the stacking conditions for the rocksalt-type sublattice, with a different monoclinic angle and, concomittantly, new centering conditions. The available experimental data are not sufficient for a proper structural refinement and new syntheses are required to improve the crystal quality of the single-crystal samples for a quantitative analysis of the diffracted intensities and a structure refinement in the framework of the present superspace symmetry considerations. However, comparison with previously known structures, and the consideration of both the crystal symmetry in the superspace approach and the metric of the crystal lattices allowed us to propose structural models and superspace groups which could be a starting point for further investigations. We could also derive some rules governing the stacking scheme of these structures, in particular concerning the structural relation between both subsystems of the misfit structure. The aperiodicity along **b** prevents any correlation in this direction, but it appears that the atomic configuration in the **a** direction keeps the same characteristics among these different phases, with a specific position of the CoO_6 octahedra sandwiched between two rocksalt-type slabs. From these considerations, we have shown that it is possible to derive a general relationship between the lattice parameters of the monoclinic unit cells characterizing these different phases and this relationship also validates the proposed structural model. Another interesting conclusion is that even if both subsystem lattices are not related to each other in the misfit direction, they keep their own coherence along the stacking direction, even in this misfit direction, so that one can really define a specific three-dimensional space group in relation to the superspace symmetry of the global aperiodic phase.

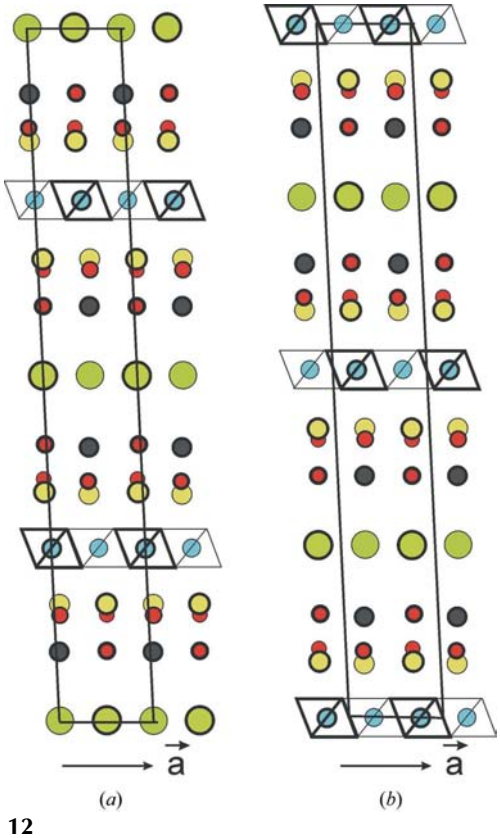

Figure 12
(*a*) First and (*b*) second structural models for $[IBi_2Ca_2O_4][CoO_2]_{1.69}$ in the $A2/m(0\delta1)s0$ symmetry. S1: thick circles: $y = 0$, thin circles: $y = 0.5$; S2: thick circles: $y = -0.25$, thin circles: $y = 0.25$.

References

Balsys, R. J. & Davis, R. L. (1996). *Solid State Ion.* **93**, 279–282.
Boullay, Ph., Seshadri, R., Studer, F., Hervieu, M., Groult, D. & Raveau, B. (1998). *Chem. Mater.* **10**, 92–102.
Duisenberg, A. J. M., Kroon-Batenburg, L. M. J. & Shreurs, A. (2003). *J. Appl. Cryst.* **36**, 220–229.
Funahashi, R., Guilmeau, E., Maeda, Y., Mikami, M. & Mihara, T. (2005). *Trans. Mater. Res. Soc. Jpn*, **30**, 523–526.
Funahashi, R., Matsubara, I. & Sodeoka, S. (2000). *Appl. Phys. Lett.* **76**, 2385–2387.
Grebille, D., Lambert, S., Bourée, F. & Petrícek, V. (2004). *J. Appl. Cryst.* **37**, 823–831.
Grebille, D., Leligny, H., Ruyter, A., Labbé, Ph. & Raveau, B. (1996). *Acta Cryst.* B**52**, 628–642.
Guilmeau, E., Mikami, M., Funahashi, R. & Chateigner, D. (2005). *J. Mater. Res.* **20**, 1002.
Guilmeau, E., Pollet, M., Grebille, D., Hervieu, M., Muguerra, H., Cloots, R., Mikami, M. & Funahashi, R. (2007). *Inorg. Chem.* **46**, 2124–2131.
Hébert, S., Lambert, S., Pelloquin, D. & Maignan, A. (2001). *Phys. Rev. B*, **64**, 172101, 1–4.
Hervieu, M., Boullay, Ph., Michel, C., Maignan, A. & Raveau, B. (1999). *J. Solid State Chem.* **142**, 305–318.

Jakubowicz, N., Grebille, D., Hervieu, M. & Leligny, H. (2001). *Phys. Rev. B*, **63**, 214511, 1–11.
Janssen, T., Janner, A., Looijenga, A. & de Wolff, P. M. (1992). *International Tables for Crystallography*, Vol. C, p. 797. Dordrecht: Kluwer Academic Publishers.
Jorgensen, J. D., Avdeev, M., Hinks, D. G., Burley, J. C. & Short, S. (2003). *Phys. Rev. B*, **68**, 214517, 1–10.
Karppinen, M., Fjellvåg, H., Konno, T., Morita, Y., Motohashi, T. & Yamauchi, H. (2004). *Chem. Mater.* **16**, 2790–2793.
Lambert, S., Leligny, H. & Grebille, D. (2001). *J. Solid State Chem.* **160**, 322–331.
Leligny, H., Grebille, D., Pérez, O., Masset, A. C., Hervieu, M. & Raveau, B. (2000). *Acta Cryst.* B**56**, 173–182.
Li, S., Funahashi, R., Matsubara, I., Ueno, K. & Yamada, H. (1999). *J. Mater. Chem.* **9**, 1659–1660.
Lynn, J. W., Huang, Q., Brown, C. M., Miller, V. L., Foo, M. L., Schaak, R. E., Jones, C. Y., Mackey, E. A. & Cava, R. J. (2003). *Phys. Rev. B*, **68**, 214516, 1–7.
Maignan, A., Hébert, S., Pi, L., Pelloquin, D., Martin, Ch., Michel, C., Hervieu, M. & Raveau, B. (2002). *Crystal Eng.* **5**, 365–382.
Maignan, A., Hébert, S., Pelloquin, D., Michel, C. & Hejtmanek, J. (2002). *J. Appl. Phys.* **92**, 1964–1967.
Maignan, A., Wang, C. B., Hébert, S., Pelloquin, D. & Raveau, B. (2002). *Chem. Mater.* **14**, 1231–1235.
Masset, A. C., Michel, C., Maignan, A., Hervieu, M., Toulemonde, O., Studer, F., Raveau, B. & Hejtmanek, J. (2000). *Phys. Rev. B*, **62**, 166–175.
Miyazaki, Y. (2004). *Solid State Ion.* **172**, 463–467.
Miyazaki, Y., Miura, T., Ono, Y. & Kajitani, T. (2002). *Jpn. J. Appl. Phys.* **41**, L849–L851.
Morita, Y., Poulsen, J., Sakai, K., Motohashi, T., Fujii, T., Terasaki, I., Yamauchi, H. & Karppinen, M. (2004). *J. Solid State Chem.* **177**, 3149–3155.
Muguerra, H. (2007). Private communication.
Nagaï, T., Sakaï, K., Karppinen, M., Asaka, T., Kimoto, K., Yamazaki, A., Yamauchi, H. & Matsui, Y. (2006). *J. Solid State Chem.* **179**, 1898–1903.
Pelloquin, D., Hébert, S., Maignan, A. & Raveau, B. (2005). *J. Solid State Chem.* **178**, 769–775.
Pelloquin, D., Maignan, A., Hébert, S., Martin, C., Hervieu, M., Michel, C., Wang, L. B. & Raveau, B. (2002). *Chem. Mater.* **14**, 3100–3105.
Pérez, O., Leligny, H., Grebille, D., Labbé, Ph., Groult, D. & Raveau, B. (1995). *J. Phys. Condens. Matter*, **7**, 10003–10014.
Petříček, V. & Dušek, M. (2000). *JANA*2000. Institute of Physics, Praha, Czech Republic.
Shizuya, M., Isobe, M., Baba, Y., Nagai, T., Matsui, Y. & Takayama-Muromachi, E. (2006). *J. Solid State Chem.* **179**, 3948–3954.
Smaalen, S. van (1992). *Mater. Sci. Forum*, **100/101**, 173–222.
Smaalen, S. van (2004). *Z. Kristallogr.* **219**, 681–691.
Smaalen, S. van & de Boer, J. L. (1992). *Phys. Rev. B*, **46**, 2750–2757.
Subramanian, M. A. (1994). *J. Solid State Chem.* **110**, 193–195.
Takada, K., Sakurai, H., Takayama-Muromachi, E., Izumi, F., Dilanian, R. A. & Sasaki, T. (2003). *Nature*, **422**, 53–55.
Terasaki, I., Sasago, Y. & Uchinokura, K. (1997). *Phys. Rev. B*, **56**, R12685–12687.
Xiang, X. D., McKernan, S., Vareka, W. A., Zettl, A., Corkill, J. L., Barbee, T. W. & Cohen, M. L. (1990). *Nature*, **348**, 145–147.
Xiang, X. D., Vareka, W. A., Zettl, A., Corkill, J. L., Kijima, N. & Gronsky, R. (1992). *Phys. Rev. Lett.* **68**, 530–533.
Yamamoto, T., Uchinokura, K. & Tsukada, I. (2002). *Phys. Rev. B*, **65**, 184434, 1–12.
Yamauchi, H., Sakai, K., Nagai, T., Matsui, Y. & Karppinen, M. (2006). *Chem. Mater.* **18**, 155–158.